

# Synthesis and Characterization of a Bi-functional Porphyrin: Electrochemical Modulation of Oxygen Binding

Richard A. Whitt and C.W. Anderson

Department of Chemistry, Hampden-Sydney College, Hampden-Sydney, VA 23943

A metalloporphyrin containing peripheral ferrocene groups was synthesized using pyrrole condensation and Heck coupling reactions. The structure of tetra(3,5-divinylferrocenylphenyl)porphyrin (Fc<sub>8</sub>-TPP) is characterized using U.V. Vis. and H<sup>1</sup>-NMR spectroscopy. Future studies on the electrochemical and oxygen binding properties of Fc<sub>8</sub>-TPP using cyclic voltammetry and other spectroelectrochemical techniques are of interest.

## INTRODUCTION

Oxygen transfer is an essential biochemical process utilized by aerobic organisms. The ability of organisms to transport oxygen is significant to the functionality of the species in terms of respiration or other evolutionary adaptations. Fish control buoyancy by an organ called a swim bladder that inflates and deflates with oxygen fed from specific carriers in its bloodstream. The biochemical mechanism by which oxygen is transferred and stored is the general subject for this study. However, the goal of this project is to synthesize a molecule that mimics biochemical oxygen modulation in aqueous media by means of electrochemically induction instead of using blood components.

The binding and unbinding of oxygen in the synthetic oxygen carrier is controlled by the transfer of electrons. Electron transfer is induced heterogeneously by the passage of the medium containing the oxygen carrier molecule across an electrode. Soon after the carrier molecule comes in contact with the electrode, a heterogeneous electron exchange between the oxygen binding site at the core of the carrier and the electron transfer sites at the periphery of the molecule can take place. The oxidation state of the carrier is monitored throughout the redox cycle. The bi-functionality of the carrier refers to its ability to transfer electrons laterally across the molecule and at a rate that allows the molecule to bind and unbind oxygen in a flow through model. This research specifically focuses on the synthesis and characterization of a porphyrin that can later be used as a synthetic oxygen carrier exhibiting the specified electrochemical properties.

Metalloporphyrins are the oxygen carrying compounds in mammalian blood. They can be found in the heme in hemoglobin which consists of a ring shaped molecule containing a core iron atom with the ability to bind oxygen. Synthetic metalloporphyrins with a central metal atom have been prepared to exhibit oxygen binding similar to the biochemical process associated with the heme.<sup>[2,3,4]</sup> Cobalt(II)-Schiff-base complexes and Collman's "picket fence porphyrins" are examples of synthetic oxygen carriers. These molecules have a nitrogenous cores similar to hemoglobin but deliver a slow uptake of oxygen measured on the order of days.<sup>[5,6]</sup> Collman's

paper is of special interest because it emphasizes the binding regions and regiospecificity of metalloporphyrin complexes. Collman's ideas become crucial when dealing with oxygen binding or potential dimerization of the porphyrin.<sup>[6]</sup> However, the most important aspect is building a molecule that will proceed with rapid heterogeneous electron transfer allowing oxygen to bind and unbind measurably within the model.

The basic structure of a porphyrin consists of four pyrrole subunits forming a ring with a nitrogenous core. The compound of interest in this study is tetraphenylporphyrin (TPP) which can be seen in comparison to the basic components of the heme in Figure 1. For the overall reaction, benzaldehyde undergoes consecutive nucleophilic addition with pyrrole to form a porphyrinogen intermediate which is then oxidized to the final porphyrin product.<sup>[20]</sup>

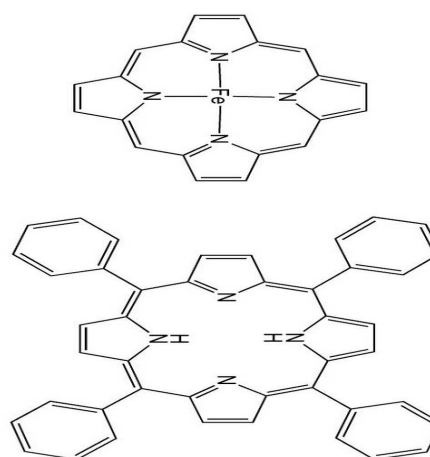


Fig1. "Heme" vs. TPP<sup>[7]</sup>

TPP can form complexes with metals such as zinc, iron, cobalt, and nickel<sup>[19]</sup> each having varying redox potentials and oxygen binding properties as porphyrins.<sup>[8,9]</sup> However, solubility of synthetic carriers may be problematic considering heme transfers oxygen in a hydrophobic environment in the bloodstream.<sup>[10]</sup>

Two synthetic routes are explored to attach vinyl ferrocenes at the meta position on the outer phenyl rings of TPP forming a new compound tetra(3,5-Divinylferrocenylphenyl) porphyrin which is referred to as Fc<sub>8</sub>-TPP. The main reaction for attaching the vinyl ferrocenes around the periphery of the porphyrin is a Heck coupling reaction, seen in Figure 2 as the first step in Approach B. After the Heck reaction, the product is used in the porphyrin condensation reaction from the Adler paper to form Fc<sub>8</sub>-TPP (Figure 3). Approach A uses a condensation reaction first to form a porphyrin intermediate before coupling vinyl ferrocene.

Fc<sub>8</sub>-TPP has not been previously reported in literature. Coordinating a metal atom in at the core of Fc<sub>8</sub>-TPP remains the final step in synthesizing an oxygen carrier molecule. Also, core metal atoms in ferrocene substituted porphyrins have not appeared in literature. Previous references show porphyrin dendrimers synthesized with peripheral vinyl ferrocenes.<sup>[12,13,14]</sup> However, the extended structure of these dendrimers compared to Fc<sub>8</sub>-TPP may be problematic considering proximity of the outer vinyl ferrocenes to the core metal atom may be crucial for the speed of electrochemical interactions within the carrier.

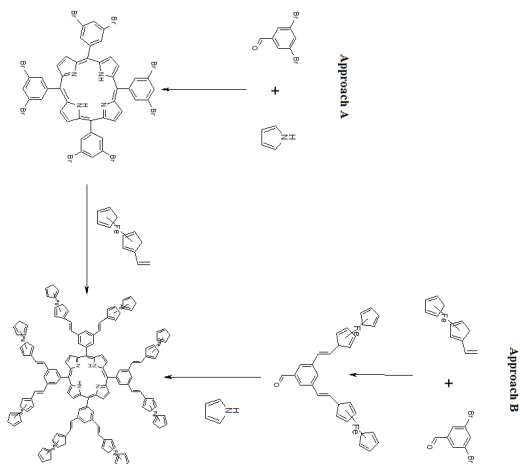


Fig2. Reaction Schemes for Synthetic Approaches

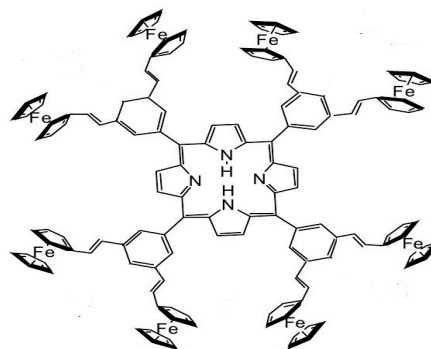


Fig3. Fc<sub>8</sub>-TPP

The vinyl ferrocenes are the electron transfer sites on the molecule. The rate constant values for metalloporphyrin reduction are 10-100 times smaller than the value measured for ferrocene.<sup>[11]</sup> Thus, as hypothesized, the faster reduction of the outer ferrocenes must be considered when constructing an electrode model to ensure electron transfer between the core atom can occur before the carrier continues along the redox cycle. In the future, cyclic voltammetry can be used to monitor the intermolecular oxidation states of specific components of the carrier.

The acid-base reaction that induces the binding and unbinding of oxygen in fish is reversible to control buoyancy and suite the organisms biological need.<sup>[1]</sup> The oxygen-carrier model used in this study exhibits similar characteristics to a swim bladder. Table 1 gives the four basic components of our model and how it relates to the components of a swim bladder.

Component	Fish	Electrode Model
Membrane	Gills	Oxygen Permeable Membrane
Oxygen Carrier Solution	Blood (Hemoglobin)	Synthetic Carrier
Pump Mechanism	Heart	Electric Pump
Control Mechanism	Acid/Base Secretions	Electrodes

Table 1. Basic Model Components

In order to unbind the oxygen from the carrier, the ferrocene molecules must come in contact with the electrode. At this point, the outer ferrocene becomes reduced, changing the oxidation state of the peripheral species from  $\text{Metal}^{3+}$  to  $\text{Metal}^{2+}$ . The peripheral species can then laterally exchange electrons with the core metal atom enabling the carrier molecule to bind oxygen.

Figure 4 is the general electrochemical mechanism behind the bi-functional synthetic carrier. The outer white circles represent the un-reduced species that become reduced when passed by the electrode. The central white square represents the un-reduced core metal atom. Once gaining an electron, the outer species can then donate an electron to the core atom reducing the metal to a state that can bind oxygen. The shaded regions represent the all reduced species. In this study, the white circles and square would indicate a +3 oxidation state considering the use of iron, while the shaded circles and square indicate a +2 oxidation state of these species. This process is reversible and can happen in both directions across the electrode.

The vinyl ferrocenes are the kinetically preferred electron transfer sites on the molecule. Thus, as proposed, the faster reduction of the outer ferrocenes must be considered when constructing an electrode model to ensure electron transfer between the core atom can occur before the carrier continues along the redox cycle. Matching the  $E^\circ$  of the central (oxygen binding) metal and the peripheral ferrocene will be important. In the future, cyclic voltammetry can be used to monitor the intermolecular oxidation states of specific components of the carrier.

The entire redox cycle of the carrier can be seen in the electrochemical model in Figure 5. Also, the binding and unbinding of oxygen between electrodes is illustrated. The rate at which the carrier central metal is (re-)reduced to an oxygen binding species must be within the amount of time it takes for the carrier to pass by the next electrode.

## METHODS

Two approaches were taken to synthesize tetra(3,5-Divinylferrocenylphenyl) porphyrin ( $\text{Fc}_8\text{-TPP}$ ). Approach A used the experimental protocol From Adler to synthesize *meso*-tetraphenylporphyrin, TPP. Freshly distilled pyrrole (56 ml, 0.8 mole) and 80 mL (0.8 mole) of reagent grade benzaldehyde was added to 3 liters of refluxing reagent grade propanoic acid. After refluxing for 30 min, the solution was cooled to room temperature and filtered, and the filter cake was then washed thoroughly with methanol. After a hot water wash, the resulting purple crystals was air dried, and finally dried *in vacuo* to remove adsorbed acid to yield 25 g (20%, yield) of TPP (Adler). The TPP was purified on silica gel using 7:1 mixture of

hexane to ethyl acetate and was characterized using UV-Vis, TLC, H-NMR, and C-NMR spectroscopy. For the synthesis of the TPP Zinc complex 1-2 mg of the TPP at room temperature was dissolved in 3 mL of dimethylformamide (DMF) in a 5-mL reaction vial containing a stir bar. Dry zinc chloride, 10 mg, is added to the vial, and the reactants are heated to a gentle reflux for 30 min. The resulting solution was diluted with DMF to measure the visible spectrum. The synthesis of  $\text{Ni}^{\text{II}}(\text{TPP})$  uses 10 mg of dry nickel(II) chloride but is otherwise identical. The synthesis of (E)-3,5-(Divinylferrocenyl)benzaldehyde<sup>[21,22,23]</sup> was carried out according to The Victoronova-Lijanov paper, which couples vinyl ferrocene in a Heck coupling reaction with 3,5-dibromo-benzaldehyde. A mixture of vinyl ferrocene, 3,5-dibromo-benzaldehyde,  $\text{Pd}(\text{OAc})_2$ , and tri-*o*-tolylphosphine POT in  $\text{Et}_3\text{N}/\text{DMF}$  1:5 (120 mL) was stirred under nitrogen at 120 C for 24 h. After cooling, the resulting mixture was filtered and the solvents evaporated. The crude product was purified by column chromatography ( $\text{SiO}_2$ , hexane) and characterized using UV-Vis and H-NMR spectroscopy.

**Synthesis of Tetra(3,5-Divinyl ferrocenylphenyl) porphyrin ( $\text{Fc}_8\text{-TPP}$ )** Using the Adler paper's porphyrin reaction, benzaldehyde is substituted with 3,5-(Divinylferrocenyl)benzaldehyde in equimolar amounts. The reaction forms dark red to brown crystals that is purified on silica gel with hexane. Using U.V.-Vis and 2D-NMR are useful in revealing porphyrin like characteristics. SEM-EDS showed multiple crystal structures within unpurified  $\text{Fc}_8\text{-TPP}$ ; however, elemental analysis confirmed the presence of electron dense, iron containing molecules.

## Experimental: Approach B

**Synthesis of Tetra(3,5-Dibromophenyl)porphyrin** The second synthetic route uses the porphyrin condensation reaction in the Adler but substitutes 3,5-Dibromobenzaldehyde for benzaldehyde in equimolar amounts. This method is used to create binding regions around the perimeter of the TPP by attaching bromine to the meta positions on the outer phenyl rings. Previous literature has TPP substituted at the beta-pyrrole position with bromine using bromination and demethylation reactions and also coordinating the compound with a central metal atom.<sup>[16,17,18,25]</sup> While several phenyl substitutions have been reported to result in successful porphyrin formation, some substitutions do not and no literature source located has reported substituting the phenyl rings with bromine. Thus, characterization is based of beta-pyrrole substituted porphyrins with bromine using H-NMR to detect variable splitting. UV-Vis spectroscopy confirmed the new compound still contained porphyrin-like characteristics yet showed varying peak intensities.

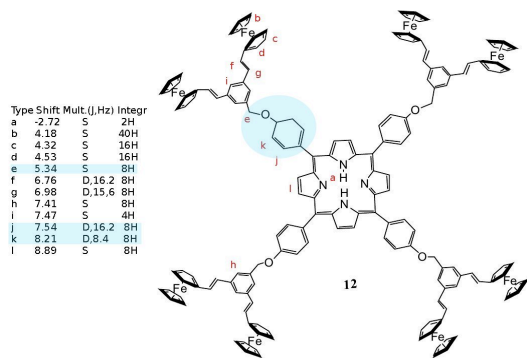
Reactants	Referenced	Experimental
Pyrrrole	*H <sup>1</sup> -NMR: 6.12(4), 6.65(4), 8.82 ppm *C <sup>13</sup> -NMR: 108.5, 118.6 ppm	H <sup>1</sup> -NMR: 6.52(4), 6.94(4), 8.1 ppm C <sup>13</sup> -NMR: 108.3, 118.2 ppm
3,5-Dibromobenzaldehyde	*H <sup>1</sup> -NMR: 7.7(3), 7.8(3), 9.8 ppm *C <sup>13</sup> -NMR: 127.0, 131.0, 138.0, 191.0 ppm	H <sup>1</sup> -NMR: 7.89(3), 7.91(3), 9.8 ppm C <sup>13</sup> -NMR: 127.0, 131.0, 139.0, 189.0 ppm
Tetraphenylporphyrin (TPP)	H <sup>1</sup> -NMR: (-2.79), 7.75, 7.77, 8.28, 8.85 ppm <sup>[26,27]</sup> U.V. Vis.: 514, 550, 590, 650 nm <sup>[9]</sup>	H <sup>1</sup> -NMR: 7.74, 7.76, 8.21, 8.84 ppm U.V. Vis.: 512, 548, 590, 643 nm
Vinyl Ferrocene	H <sup>1</sup> -NMR: 4.1, 4.2(3), 4.3(3), 5.0(3), 5.3(3), 6.3-6.5(4) ppm <sup>[28]</sup>	H <sup>1</sup> -NMR: 4.09, 4.20(3), 4.35(3), 5.0(3), 5.3(3), 6.4(4) ppm
3,5-(Divinylferrocenyl) benzaldehyde	H <sup>1</sup> -NMR: 4.16, 4.32, 4.50, 6.75(2), 7.02(2), 7.65, 7.79, 10.05 ppm <sup>[13]</sup> U.V. Vis.: 248, 314, 458 nm <sup>[13]</sup>	H <sup>1</sup> -NMR: 4.14, 4.32(3), 4.50(3), 6.75(2), 7.00(2), 7.64, 7.79, 10.03 ppm U.V. Vis.: 250, 312, 457 nm
Tetra(3,5-Dibromophenyl) porphyrin	N/A	H <sup>1</sup> -NMR: 7.52(4), 7.70(4), 8.12, 8.90 ppm U.V. Vis.: 512, 591, 626, 656 nm

Table 2: Spectral Data Summary (\*Produced from NMR spectra generator software)<sup>[29]</sup>

## RESULTS AND DISCUSSION

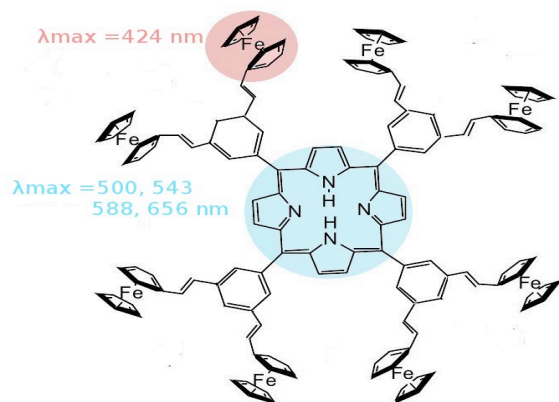
The characterization of tetra(3,5-dibromophenyl)porphyrin and Fc<sub>8</sub>-TPP is difficult considering no references have been found on either compounds. The low yield and formation of various undesired products made the thorough characterization of tetra(3,5-dibromophenyl)porphyrin difficult also. Historically, porphyrins typically yield in the 25-40% range as it is, so a low yield was expected. These problems with Approach A led us to Approach B, a new synthetic route for making Fc<sub>8</sub>-TPP. Conceptually, both approaches use the same types of reactions but in a different order.

The Morales-Espinoza paper has H<sup>1</sup>-NMR and U.V. Vis. data of a polyferrocenyl dendrimer with a porphyrin core referred to as Dendrimer 12 seen in Figure 4.

Fig4. Dendrimer 12<sup>[21]</sup>

Dendrimer 12's UV-Vis and proton spectrum will be similar to Fc<sub>8</sub>-TPP in that it contains shifts indicative of both TPP and 3,5-(Divinylferrocenyl)benzaldehyde. This is useful for analyzing Fc<sub>8</sub>-TPP because Dendrimer 12 has the same spectrally active sites, especially for UV-Vis, giving rise to hypothetically similar chemical shifts and absorbance patterns for Fc<sub>8</sub>-TPP. The peaks that are highlighted in blue in Figure 8 are from proton environments that should not present in Fc<sub>8</sub>-TPP's proton spectrum.

In Figure 5, the highlighted areas are the spectrally active sites that are in common between Dendrimer 12 and Fc<sub>8</sub>-TPP. The sampling method and slightly different compound structure can account for variability in wavelengths. What is important is that the shifts in wavelengths stayed consistent within the spectrum and both active sites are represented.

Fig5. Fc<sub>8</sub>-TPP Spectrally Active Sites

A method of purifying and characterizing TPP and tetra(3,5-dibromophenyl)porphyrin simultaneously was used by placing a flow through cuvette in the U.V. Vis. spectrometer and having the eluent from the column run through the cuvette. A spectrum was taken every 5-10 seconds mapping out the absorption of the material passing through the spectrometer. Figure 6 is an overlaid U.V. Vis. spectrum of TPP separated with a silica column. Notice the change in peak intensities correlating to the concentration of TPP flowing through the cuvette from the column at different times.

There is a similarity between tetra(3,5-dibromophenyl)porphyrin and TPP that can be seen by the overall absorbance pattern. The major difference between the spectrum in Figure 7 and 8 is the shift in absorbance to higher wavelengths for tetra(3,5-dibromophenyl)porphyrin. The spectrum shows the structural integrity of the porphyrin remains; however, it suggests the compound has electronic transitions that are different compared to TPP due to bromination.

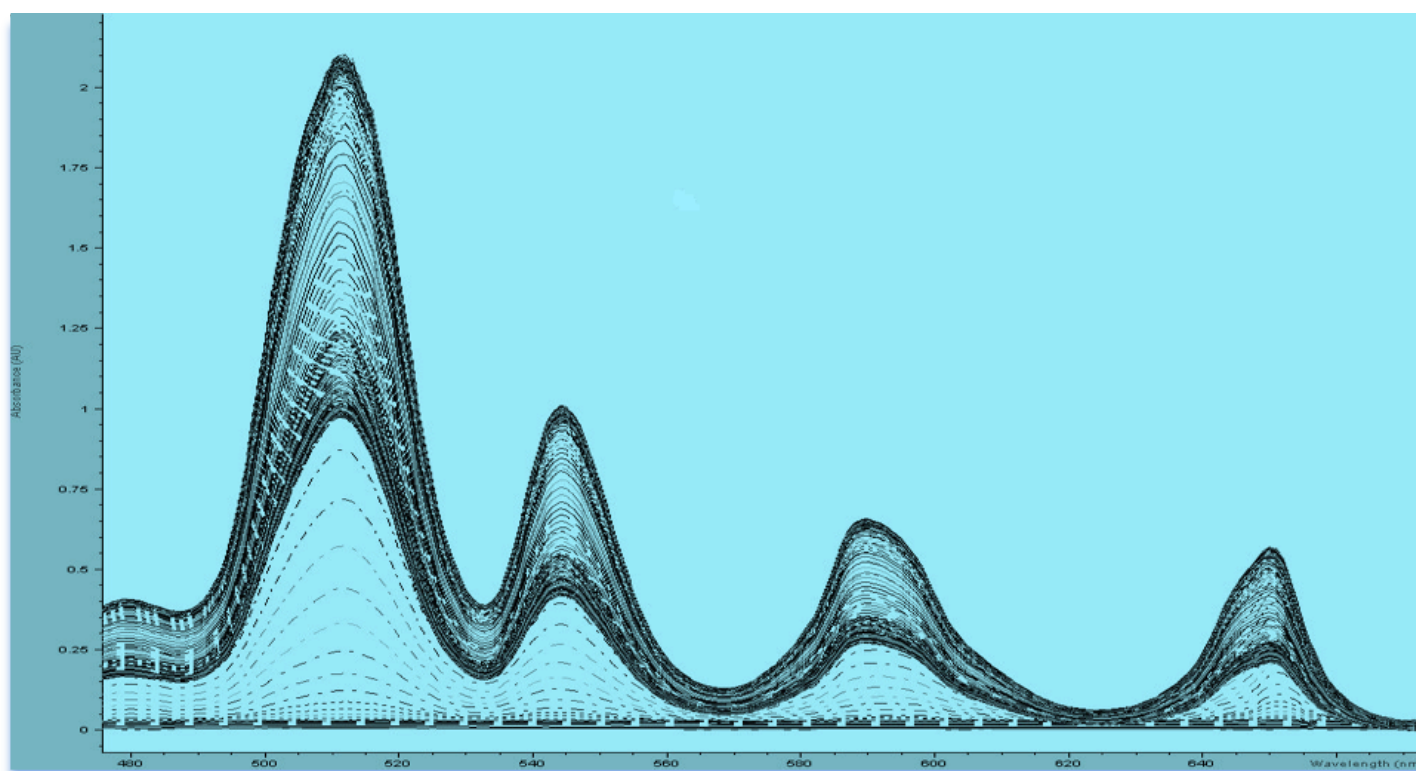


Figure 6. Column Chromatography coupled U.V. Vis. Spectrum of TPP

Figure 7 is an overlaid U.V.-Vis spectrum of purified 3,5-(divinylferrocenyl) benzaldehyde. The UV-Vis spectrum of Fc<sub>8</sub>-TPP should hypothetically exhibit characteristics of both TPP and 3,5-(divinylferrocenyl)benzaldehyde and be easily detected since both absorb in different regions. We should not see any absorbance peaks pass the 450

nm range indicative of any porphyrin formation in Figure 7. Figure 8 is the visible spectrum of Fc<sub>8</sub>-TPP which has absorbencies correlating with TPP and 3,5-(divinylferrocenyl)benzaldehyde as predicted. Notice the 4 peaks that arise beyond the 450 nm range that correlate to porphyrin formation. A few data points were caused by noise giving rise to illegitimate peaks, but did not affect the overall spectrum. Figure 8 is

conclusive data for the formation of  $\text{Fc}_8\text{-TPP}$ ; however, a better sample size would improve my spectrum. The overall yield is  $<0.1$  g of red-orange solid. Since the sample size was so small after being purified, NMR characterization was insufficient due to such a low yield. UV-Vis worked well because the compound absorbs at very low concentration; however, a more adequate sample is needed for a full NMR workup.

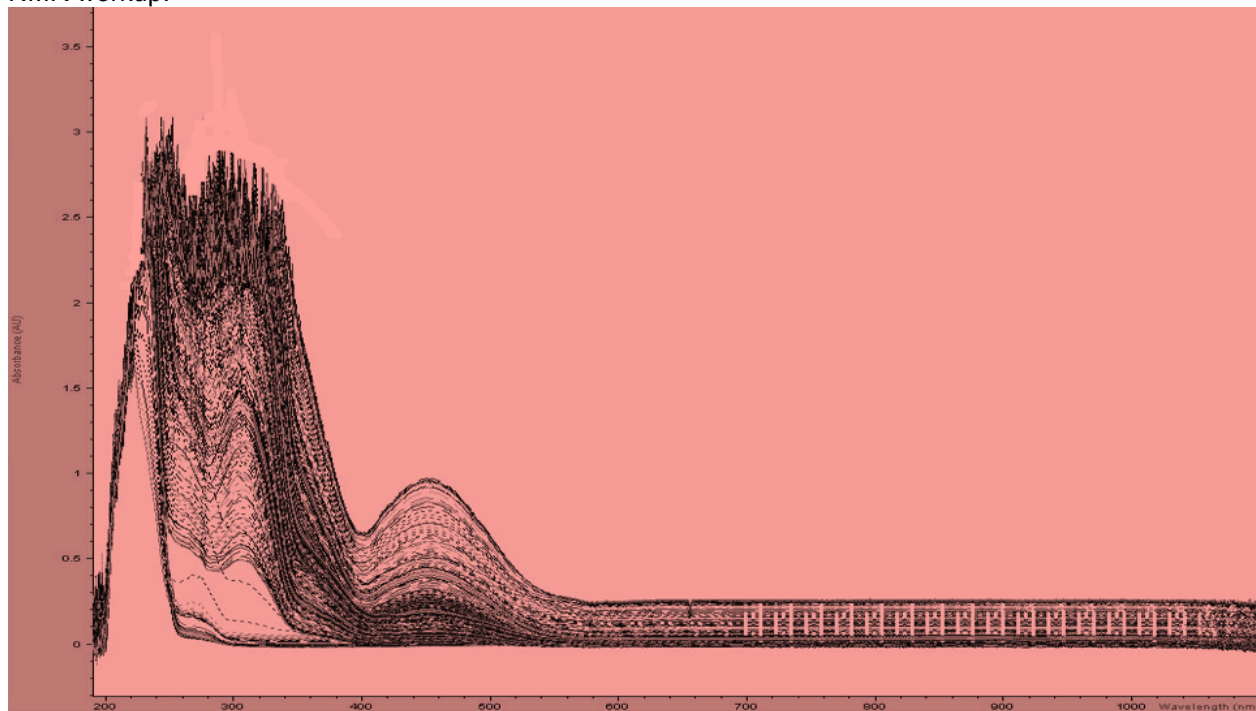


Figure 7. UV-Vis Spectrum of 3,5-(Divinylferrocenyl)benzaldehyde

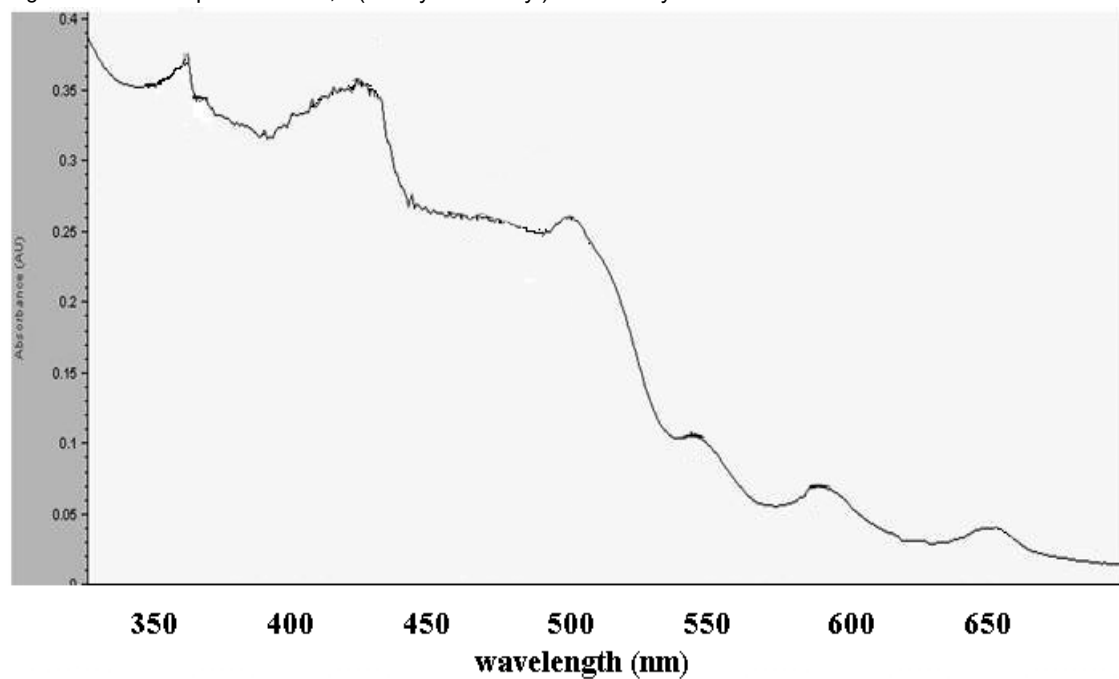
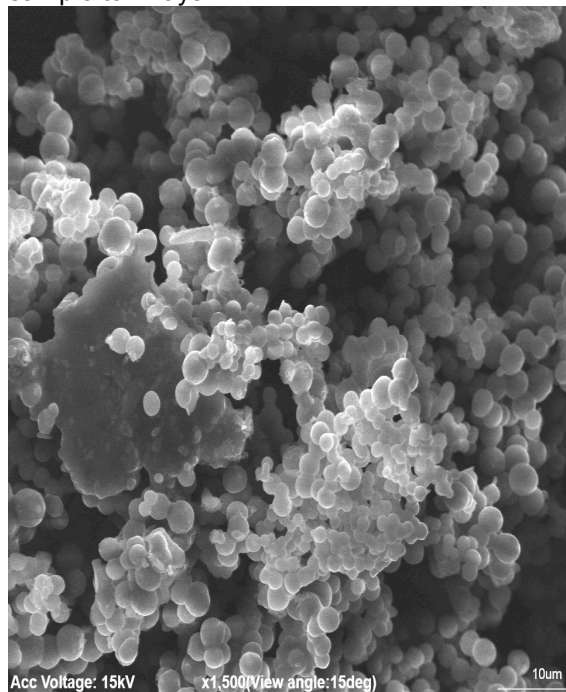


Figure 8. UV-Vis Spectrum of  $\text{Fc}_8\text{-TPP}$ 

Scanning Electron Microscopy (SEM) coupled with Energy Dispersive X-ray Spectroscopy (EDS) allowed for a high resolution, high magnification picture of unpurified  $\text{Fc}_8\text{-TPP}$  seen in Figure 9. Spectroscopy was performed at Pittcon in Orlando, which at the time only we only had an unpurified product. Two distinct crystal structures are clearly visible from this sample in this micrograph.

The brighter regions around the spheres within the major crystal lattice to the right represent areas of higher electron density possibly correlating to the presence of peripheral ferrocenes. From this image, a  $10 \times 10 \mu\text{m}$  section is cropped and highlighted for EDS. EDS allows for an elemental analysis based on the energy difference between excited states and ground states after introducing the sample to x-rays.

Fig 9. Scanning Electron Micrograph of  $\text{Fc}_8\text{-TPP}$ <sup>29</sup>

## REFERENCES

1. Junqwi, Megan. *How Fish Maintain Buoyancy*. Sept. 7, 2005. "<http://www.suite101.com/http://www.suite101.com/content/how-fish-maintain-buoyancy-a149439>."
2. Bhyrappa, P.; Sankar, M.; Varghese, B. *Inorg. Chem.* 2006, 45, 4136-4149.
3. Bhyrappa, P.; Arunkumar C.; Varghese, B. *Inorg. Chem.* 2009, 48, 3945-3965.
4. Chen, J.; Zhang, Weiman. *Chem. Commun.* 2007, 3353-3355.
5. Basolo, Fred; Hoffman, Brian M.; Ibers, James A. *Acc. Chem. Res.*, 8, 384-392 (1975).
6. Collman, James P.; Grange, Robert R.; Reed, Christopher A. *Journal of the American Chemical Society*. 1975, 97, 1427-1439.
7. Santa Cruz Biotechnology. *Meso-Tetraphenylporphyrin*: sc-215304. "<http://www.scbt.kr/datasheet->" "<http://www.scbt.kr/datasheet-215304-meso-tetraphenylporphyrin.html>."
8. Walker, Ann. *Journal of the American Chemical Society*. 1973, 95, 1154-1159.
9. Marsh, Diane; Mink, Larry M.; *Journal of Chemical Education*. 1996, 73, 1188-1190.
10. Angelini, Nicola; Micali, Norberto; Mineo, Placido. *J. Phys. Chem.* 2005, 109, 18645-18651.
11. Feng, Diwei; Schultz, Franklin A. *Inorg. Chem.* 1988, 27, 2144-2149.
12. Morales-Espinoza, Eric G.; Sanchez-Montez, Karla E. *Molecules*. 2004, 15, 2564-2575.
13. Victorovna-Lijanova, Irina; reyes-Valderrama, Maria I. *Tetrahedron*. 2008, 64 (19), 4460-4467.
14. Nemykin, Victor N.; Rohde, Gregory T. *Inorg. Chem.* 2010, 49, 7494-7509.
15. Alan D. Adler, Frederick R. Longo, John D. Finarelli, Joel Goldmacher, Jacques Assour, Leonard Korsakoff. *The Journal of Organic Chemistry* 1967, 32 (2), 476-476.
16. Bhyrappa P.; Krishnan V.; *Inorg. Chem.* 1991, 30, 239-245.
17. Crossley, Maxwell J.; Burn, Paul L.; Chew, Sioe See; Cuttance, F. Brett. *J. Chem. Soc., Chem. Commun.*, 1991, 1564-1566.
18. Senge, Mathias O.; Gerstung, Vanessa; Ruhlandt-Senge, Karin; Runge, Steffen; Lehman, Ingo. *J. Chem. Soc., Dalton Trans.*, 1998, 4187-4199
19. Toshie Ohya and Mitsuo Sato. *Bull. Chem. Soc. Jpn.*, 69, 3201-3205 (1996).
20. Harwood, Laurence M.; Moody, Christopher J.; *Experimental Organic Chemistry*. Blackwell Scientific Publications: Oxford, 1989.
21. Morales-Espinoza, Eric G.; Sanchez-Montez, Karla E. *Molecules*. 2004, 15, 2564-2575.
22. Victorovna-Lijanova, Irina; reyes-Valderrama, Maria I. *Tetrahedron*. 2008, 64 (19), 4460-4467.
23. Kantchev, Eric Assen B.; Peh, Guang-Rong; Zhang, Chi; Ying, Jackie Y. *Org. Lett.* 2008, 10, 3949-3952.
24. Wheeler, Julia R. *Spectroelectrochemical Investigations of Biological Redox Molecules*. Duke University. 126-127 (1985).
25. Callot, H. J. *Bulletin De La Societe Chimique De France*. 1974, 7-8, 1492-1497.
26. Falvo, RaeAnne E.; Mink, Larry M.; Marsh, Diane F. *Journal of Chemical Education*. 1999, 76, 237-239.
27. La Mar, Gerd N.; Walker, Ann F. *Journal of the American Chemical Society*. 1973, 95, 1790-1796.
28. Rausch, M. D.; Siegel, A. *Journal of Organometallic Chemistry*. 1969, 17, 117-125.

29. Advanced Chemistry Development, Inc., HNMR Spectrum Generator: Toronto, Ontario, Canada, 2000.